

Three-dimensional micro-/nano-structuring via direct write polymerization with picosecond laser pulses

Mangirdas Malinauskas,^{1,3} Paulius Danilevičius,¹ and
Saulius Juodkazis^{2,*}

¹ *Laser Nanophotonics Group, Laser Research Center, Department of Quantum Electronics,
Physics Faculty, Vilnius University, Sauletekio ave. 10, LT-10223 Vilnius, Lithuania*

² *Centre for Micro-Photonics, Faculty of Engineering and Industrial Sciences, Swinburne
University of Technology, Hawthorn, VIC, 3122, Australia*

³ *mangirdas.malinauskas@ff.vu.lt*

**sjuodkazis@swin.edu.au*

<http://www.lasercenter.vu.lt>

<http://www.swinburne.edu.au/engineering/cmp/>

Abstract: We demonstrate capability to structure photo-polymers with sub-wavelength resolution, $\sim 200 - 500$ nm, and retrieve three-dimensional (3D) structures using a picosecond laser exposure. This alternative to commonly used ultra-short femtosecond lasers extends accessibility of 3D direct write. A popular hybrid sol-gel resist SZ2080 was used for quantitative determination of structuring resolution at 1064 nm and 532 nm wavelengths and for pulses of 8-25 ps duration at the repetition rates of 0.2 - 1 MHz. Systematic study of feature size dependence of 3D suspended nano-rods shows that linear power dependence of photopolymerization on the dose-per-pulse becomes dominant at higher repetition rates (≥ 0.5 MHz) while the two-photon nonlinear absorption is still distinguishable at rates lower than 0.2 MHz and shorter pulses (≤ 8 ps). Thermal accumulation defines polymerization when cooling time of the focal volume is larger than separation between pulses. Photopolymerization and its scaling mechanisms, quality, and fidelity at tight focusing of fs-, ps-, and cw-laser radiation are revealed and explained. 3D scaffolds for biomedicine and microlenses for optical applications are fabricated by the ps-laser direct write.

© 2011 Optical Society of America

OCIS codes: (140.3390) Laser materials processing; (220.4000) Microstructure fabrication; (350.3850) Materials processing; (160.4236) Nanomaterials.

References and links

1. S. Maruo, O. Nakamura, and S. Kawata, "Three-dimensional microfabrication with two-photon-absorbed photopolymerization," *Opt. Lett.* **2**, 132–134 (1997).
2. Y. L. Zhang, Q. D. Chen, H. Xia, and H. B. Sun, "Designable 3D nanofabrication by femtosecond laser direct writing," *Nano Today* **5**, 435–448 (2010).

3. M. Farsari and B. N. Chichkov, "Materials processing: two-photon fabrication," *Nat. Photonics* **3**, 450–452 (2009).
4. S. Juodkazis, V. Mizeikis, and H. Misawa, "Three-dimensional microfabrication of materials by femtosecond lasers for photonics applications," *J. Appl. Phys.* **106**, 051101 (2009).
5. A. Ostendorf and B. N. Chichkov, "Two-photon polymerization: a new approach to micromachining," *Photonics Spectra* **40**, 72–80 (2006).
6. F. Qi, Y. Li, D. Tan, H. Yang, and Q. Gong, "Polymerized nanotips via two-photon photopolymerization," *Opt. Express* **15**, 971–976 (2007).
7. S. Juodkazis, V. Mizeikis, K. K. Seet, M. Miwa, and H. Misawa, "Two-photon lithography of nanorods in SU-8 photoresist," *Nanotechnol.* **16**, 846–849 (2005).
8. I. Sakellari, A. Gaidukeviciute, A. Giakoumaki, D. Gray, C. Fotakis, M. Farsari, M. Vamvakaki, C. Reinhardt, A. Ovsianikov, and B. N. Chichkov, "Two-photon polymerization of titanium-containing sol-gel composites for three-dimensional structure fabrication," *Appl. Phys. A* **100** 359–364 (2010).
9. R. J. Narayan, C. Jin, A. Doraiswamy, I. N. Mihailescu, M. Jelinek, A. Ovsianikov, B. Chichkov, and D. B. Chrisey, "Laser processing of advanced bioceramics," *Adv. Eng. Mater.* **7** 1083–1098 (2005).
10. A. Ovsianikov, M. Malinauskas, S. Schlie, B. Chichkov, S. Gittard, R. Narayan, M. Löbner, K. Sternberg, K.-P. Schmitz, and A. Haverich, "Three-dimensional laser micro- and nano-structuring of acrylated poly(ethylene glycol) materials and evaluation of their cytotoxicity for tissue engineering applications," *Acta Biomater.* **7**, 967–974 (2011).
11. M. Malinauskas, V. Purlys, A. Žukauskas, G. Bičkauskaitė, T. Gertus, P. Danilevičius, D. Paipulas, M. Rutkauskas, H. Gilbergs, D. Baltrikienė, L. Bukelskis, R. Širmenis, V. Bukelskienė, R. Gadonas, V. Sirvydis, and A. Piskarskas, "Laser two-photon polymerization micro- and nanostructuring over a large area on various substrates," *Proc. SPIE* **7715** 77157F-1, (2010).
12. M. Malinauskas, A. Žukauskas, V. Purlys, K. Belazaras, A. Momot, D. Paipulas, R. Gadonas, A. Piskarskas, H. Gilbergs, A. Gaidukevičiūtė, I. Sakellari, M. Farsari, and S. Juodkazis, "Femtosecond laser polymerization of hybrid/integrated micro-optical elements and their characterization," *J. Opt.* **12**, 124010 (2010).
13. A. Ovsianikov, Gaidukevičiūtė, B. N. Chichkov, M. Oubaha, B. D. MacCraith, I. Sakellari, A. Giakoumaki, D. Gray, M. Vamvakaki, M. Farsari, and C. Fotakis, "Two-photon polymerization of hybrid sol-gel materials for photonics applications," *Laser Chem.* **2008**, 493059 (2008).
14. M. Malinauskas, H. Gilbergs, A. Žukauskas, V. Purlys, D. Paipulas, and R. Gadonas, "A femtosecond laser induced two-photon photopolymerization technique for structuring microlenses," *J. Opt.* **12**, 035204 (2010).
15. C. Schizas, V. Melissinaki, A. Gaidukevičiūtė, C. Reinhardt, C. Ohrt, V. Dedoussis, B. Chichkov, C. Fotakis, M. Farsari, and D. Karalekas, "On the design and fabrication by two-photon polymerization of a readily assembled micro-valve," *Int. J. Adv. Manuf. Technol.* **48**, 435–441 (2010).
16. A. Ovsianikov, A. Doraiswamy, R. Narayan, and B. N. Chichkov, "Two-photon polymerization for fabrication of biomedical devices," *Proc. SPIE* **6465**, 64650O (2007).
17. S. Maruo and K. Ikuta, "Three-dimensional microfabrication by use of single-photon-absorbed polymerization," *Appl. Phys. Lett.* **76** 2656–2658 (2000).
18. I. Wang, M. Bouriau, P. L. Baldeck, C. Martineau, and C. Andraud, "Three-dimensional microfabrication by two-photon-initiated polymerization with low-cost microlaser," *Opt. Lett.* **27** 1348–1350 (2002).
19. M. Thiel, J. Fischer, G. von Freymann, and M. Wegener, "Direct laser writing of three-dimensional submicron structures using a continuous-wave laser at 532 nm," *Appl. Phys. Lett.* **97** 221102 (2010).
20. A. Pikulin and N. Bityurin, "Spatial resolution in polymerization of sample features at nanoscale," *Phys. Rev. B* **75**, 195430 (2009).
21. M. Malinauskas, A. Žukauskas, G. Bičkauskaitė, R. Gadonas, and S. Juodkazis, "Mechanisms of three-dimensional structuring of photo-polymers by tightly focussed femtosecond laser pulses," *Opt. Express* **18**, 10209–10221 (2010).
22. S. Juodkazis, Y. Nishi, H. Misawa, V. Mizeikis, O. Schecker, R. Waitz, P. Leiderer, and E. Scheer, "Optical transmission and laser structuring of silicon membranes," *Opt. Express* **17**, 15308–15317 (2009).
23. A. Marcinkevičius, V. Mizeikis, S. Juodkazis, S. Matsuo, H. Misawa, "Effect of refractive index-mismatch on laser microfabrication in silica glass," *Appl. Phys. A* **76**, 257–260 (2003).
24. J. Morikawa, A. Orie, T. Hashimoto, and S. Juodkazis, "Thermal diffusivity in femtosecond-laser-structured micro-volumes of polymers," *Appl. Phys. A* **98**, 551–556 (2009).
25. M. Beresna, T. Gertus, R. Tomasiunas, H. Misawa, and S. Juodkazis, "Three-dimensional modeling of the heat-affected zone in laser machining applications," *Laser Chem.* **2008**, 976205 (2008).
26. N. Murazawa, S. Juodkazis, H. Misawa, and K. Kamada, "Two-photon excitation of dye-doped liquid crystal by a cw-laser irradiation," *Mol. Cryst. Liq. Cryst.* **489**, 310–319 (2008).
27. M. P. Hernández-Garay, O. Martínez-Matos, J. G. Izquierdo, M. L. Calvo, P. Vaveliuk, P. Cheben, and L. Banares, "Femtosecond spectral pulse shaping with holographic gratings recorded in photopolymerizable glasses," *Opt. Express* **19**, 1516–1527 (2011).
28. S. Nolte, M. Will, J. Burghoff, and A. Tünnermann, "Femtosecond waveguide writing: a new avenue to three-dimensional integrated optics," *Appl. Phys. A* **77**, 109–111 (2003).

29. W. Gawelda, D. Puerto, J. Siegel, A. Ferrer, A. Ruiz de la Cruz, H. Fernandez, and J. Solis, "Ultrafast imaging of transient electronic plasmas produced in conditions of femtosecond waveguide writing in dielectrics," *Appl. Phys. Lett.* **93**, 121109 (2008).
 30. G. Cheng, K. Mishchik, C. Mauclair, E. Audouard, and R. Stoian, "Ultrafast laser photoinscription of polarization sensitive devices in bulk silica glass," *Opt. Express* **17**, 9515–9525 (2009).
 31. D. Day and M. Gu, "Microchannel fabrication in PMMA based on localized heating by nanojoule high repetition rate femtosecond pulses," *Opt. Express* **13**, 5939–5946 (2005).
 32. L. Shah, A. Arai, S. Eaton, and P. Herman, "Waveguide writing in fused silica with a femtosecond fiber laser at 522 nm and 1 MHz repetition rate," *Opt. Express* **13**, 1999–2006 (2005).
 33. J. Siebenmorgen, K. Petermann, G. Huber, K. Rademaker, and S. Nolte, and A. Tünnermann, "Femtosecond laser written stress-induced Nd:Y₃Al₅O₁₂(Nd:YAG) channel waveguide laser," *Appl. Phys. B* **97**, 251–255 (2009).
 34. K. K. Seet, S. Juodkazis, V. Jarutis, and H. Misawa, "Feature-size reduction of photopolymerized structures by femtosecond optical curing of SU-8," *Appl. Phys. Lett.* **89**, 024106 (2006).
-

1. Introduction

During past decade direct laser writing became a popular technique of three-dimensional (3D) fabrication of micro-/nano-structures. Photopolymerization by direct write [1] has demonstrated fabrication of complex 3D and 2D objects of dimensions required for practical applications with feature sizes ranging from tens-of-nanometers to micrometers and has proven efficient despite being a serial method [2–4]. The strength of this method is reflected by the following key features: a possibility to make 3D complex objects with no geometrical restrains [5], to reach resolution on a molecular scale [6, 7], to structure flexible materials accessing tunability of refractive index [8], to apply it to biocompatible [9] and biodegradable polymers [10], to mention some of promising directions. Building functional structures by direct laser write over large areas with micro/nanoscale resolution of different materials [11] with integration of optical functions [12] opens an opportunity to apply this technology for practical uses and, in some applications, challenge established lithographic technologies.

Some of the promising applications in photonics [13], micro-optics [14], micro-fluidics [15] and biomedicine [16] are demonstrated with ultra-short laser pulses. However, by exploiting a threshold character of photo-modification, material's optical and thermal properties, together with tight focusing (with numerical aperture of objective lens $NA > 0.5$), a 3D structuring is already demonstrated over wide range of pulse durations including continuous wave (cw)-laser and for the wavelength within the direct absorption of material [17–19]. This highlights necessity of better understanding of the fundamental mechanisms of polymerization via percolation of chemical bonding under employed exposure conditions in a particular photo-material [20]. Recently, a systematic study of the photopolymerization and cross-linking mechanisms in sol-gel resist SZ2080 (or Ormosil, which is similar to Ormocer) under low laser repetition conditions, when thermal accumulation is absent, showed the dominance of avalanche excitation which appears as an one-photon process under power law scrutiny [21]. Thermal accumulation has to be addressed next for longer pulses and high repetition rates widely used in photopolymerization.

Here, we demonstrate photopolymerization of sol-gel SZ2080 resist using a low-cost picosecond laser and commercial photoinitiators. Systematic study of resolution dependence on pulse duration and pulse repetition rate has been carried out at different wavelengths to reveal the power scaling and thermal effects of photopolymerization. Thermal accumulation governs polymerization when repetition rate is larger than the cooling time of the focal volume. Change of polymerization response from nonlinear to linear is found with increasing repetition rate (due to thermal accumulation) and at increasing pulse duration. The linear power law is explained by comparison of polymerization by laser pulses of different durations.

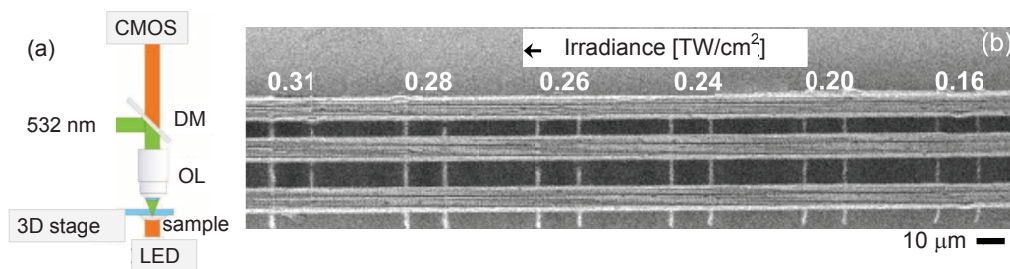


Fig. 1. (a) Schematics of direct write; DM - dichroic mirror coupler, OL - objective lens. (b) SEM image of 3D suspended resolution bridges: lines between supporting walls. Structures were fabricated by 532 nm/8 ps pulses at 1 MHz repetition rate under $NA = 1.4$ focusing; material SZ2080 with THIO photo-initiator. The irradiance at the focus is indicated.

2. Experimental

2.1. Picosecond-laser fabrication setup

We used a diode-pumped picosecond Nd:YVO laser with cavity dumping (Ekspla Ltd.). The fundamental 1064 nm and 532 nm frequency-doubled wavelengths were used for fabrication. Pulse duration and repetition rates were varied from 8 to 25 ps and from 0.2 to 1 MHz, respectively (Fig. 1(a)). Shutter-controlled ps-laser beam is coupled to an objective lens by dichroic mirror and focused into a photopolymer sample. Irradiance/intensity and pulse energy are given at the focal spot. The sample is fixed on 3D linear scanning stages (Aerotech Inc.): XY-ALS130-100 and Z-ALS130-5. These stages provide high translation speed up to 300 mm/s, and large processing area: 10 cm in lateral XY-plane and a 5 cm stroke along Z-axis. Light emitting diode (LED) provides illumination needed for CMOS-camera to in-situ monitor the fabrication sequence. Entire process of direct write is automated by a custom made *3DPoli* software. Structure patterns can be preprogrammed or imported directly from 3D CAD model. Samples were scanned at velocity $v = 100 \mu\text{m/s}$ (for bio-scaffolds at 300 $\mu\text{m/s}$).

2.2. Photosensitive polymer material

The same hybrid (organic-inorganic) pre-polymer material SZ2080 (supplied by FORTH, Heraklion) studied earlier under fs-laser exposure [21] was used for 3D structuring by ps-laser pulses. Depending on excitation wavelength used, pre-polymer is mixed with photoinitiators of 1 wt% *2,4-Diethyl-9H-thioxanten-9-one* (THIO) which has an absorption maximum at 255 nm or with 2 wt% *4,4-Bis(diethylamino)benzophenone* (BIS) with absorption maximum at 368 nm (Sigma-Aldrich GmbH) for structuring at 532 nm and 1064 nm, respectively. Methyl isobutyl ketone was used as a developer. Prepared material was drop casted on a cover glass and mounted on the sample holder for laser write. Exposed liquid pre-polymer undergoes cross-linking reaction and becomes solid and insoluble in a developer (a negative resist).

3. Results and discussion

3.1. Resolution measurement

Resolution of the structure fabricated by direct laser write is determined by focusing, energy delivery, and material response. Heat diffusion and accumulation are also important as they can cause (or contribute) to cross-linking and polymerization. In order to control thermal effects induced by laser pulses, a laser pulse pedestal (the pre- and after-pulse of an amplified

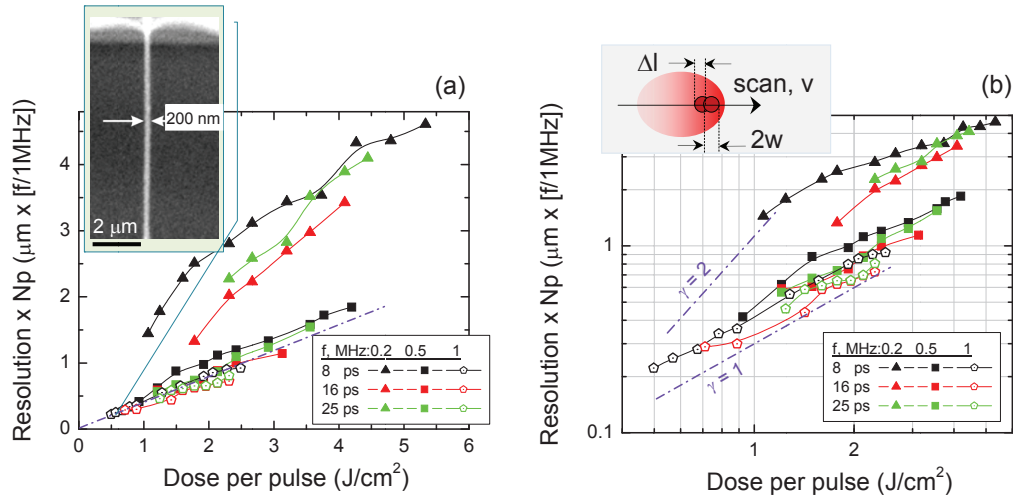


Fig. 2. Scaling mechanism of polymerization by ps-laser pulses in linear (a) and logarithmic (b) presentations. The resolution (the feature size) multiplied by the relative number of pulses per focal spot, $N_p = \frac{2w}{v/f}$, vs dose per single pulse at different repetition rates, f , and pulse durations, τ_p ; where $2w = 1.22\lambda/NA$ is the spot size at focus, $\lambda = 532$ nm is laser wavelength, $NA = 1.4$ is the numerical aperture; γ is the scaling exponent of the power law, $\Delta l = v/f$ is the overlap of the pulses along scan. Scanning velocity was $v = 100$ $\mu\text{m/s}$. The inset in (a) shows the high-resolution 3D suspended line fabricated by 8 ps pulses at 0.5 MHz; in (b) schematics of the direct write with the heat diffusion halo region.

fs-/ps-laser pulse which is tens-of-ns long) should be canceled and only the effects caused by a selected laser pulse are investigated. For that aim, we used the second harmonic (at $\lambda = 532$ nm) of the fundamental laser wavelength to exclude effects of the pulse-pedestal, which can be significant as observed in Si membrane ablation by fs-pulses at the fundamental wavelength [22]. Note, polymerization itself is an exothermic process facilitating heat accumulation.

Figure 1(b) shows SEM images of the resolution bridges used to determine the lateral resolution, a width of the bridge. Experiments were performed with different laser pulse durations, τ_p , and repetition rates, f . Structures were fabricated at different pulse energy, $E_p = P/f$, where P [W] is average laser power; the corresponding irradiance is $I = \frac{E_p}{\tau_p \pi w^2}$ [W/cm^2], here τ_p is the pulse duration, $w = 0.61\lambda/NA$ is the waist (radius) of the beam.

In order to compare resolution of the structures recorded at different pulse durations and repetition rates the following data presentation shown in Fig. 2 is chosen; linear (a) and logarithmic (b) plots are presented to better reveal the mechanisms. The width of the resolution bridge, the resolution, depends on an overlap of laser pulses which can be calculated as $N_p = \frac{2w}{v/f}$. It is defined by the repetition rate at the constant scan speed. At the 1 MHz rate, there were 5 times more pulses per focal spot $2w$ as compared with 0.2 MHz case. The resolution multiplied by the factor $\frac{f}{1[\text{MHz}]}$ was used for the ordinate axis, while the energy dose per pulse is presented on the abscise. Such presentation allows to compare resolution independently of pulse duration and laser repetition rate. Measurement of a transmitted power as a function of the incident power would provide a direct measure of the scaling power law, however, it is not always reliable at tight focusing due to presence of spherical aberration [23]. For practical reasons, it is usual to measure structure parameters of the photopolymerized structures as function of incident pulse

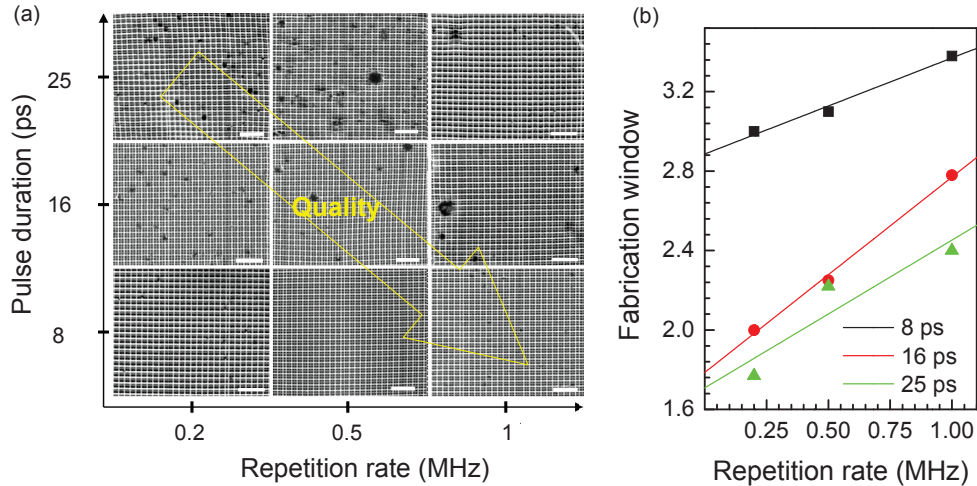


Fig. 3. Quality and fidelity of photopolymerization. (a) Qualitative comparison: SEM images of photonic crystal structures fabricated with different pulse durations and repetition rates. Scale bars, $10\ \mu\text{m}$. Arrow marks direction for the quality and fidelity increase. (b) Fidelity measure of fabrication: the fabrication window $FW = \frac{P_d}{P_{th}}$, here P_d is the optical damage power/irradiance and P_{th} is the polymerization threshold.

energy/fluence/irradiance or dose and indirectly determine the power scaling.

The highest resolution single bridges of $\sim 200\ \text{nm}$ width were recovered after development and rinse. The high repetition rate is essential to retrieve good quality (discussed below) and high resolution structures. Reproducibility of 25% of patterns after development was taken as a threshold value for a successful structuring. There is a distinctive difference between the resolution of structures fabricated at 0.2 MHz with those at 0.5 and 1 MHz. This highlights the difference in thermal accumulation and local temperature. Typical temperature diffusion constant of polymers is $\chi \simeq 1.1 \times 10^{-7}\ \text{cm}^2/\text{s}$ [24]. At the repetition rate of $f = 1\ \text{MHz}$ the diffusion length is $L_D = \sqrt{\chi \times \frac{1}{f}} \simeq 332\ \mu\text{m}$. The heat affected region extends around and ahead irradiation spot during scanning [25] as schematically shown in the inset of Fig. 2(b). Thermal accumulation becomes important when the cooling time of the irradiated spot, $t_c = (2w)^2/\chi$, is comparable with the time separation between consequent pulses; e.g., at a $NA = 1.4$ focusing $t_c \simeq 2\ \mu\text{s}$ and the temporal pulse separation is $1/f$. Only in the case of $f = 0.2\ \text{MHz}$, $t_c < 1/f$ and distinct change of the power scaling is observed due to the absence of thermal accumulation.

Change of the polymerization from partly nonlinear process to the linear is revealed in Fig. 2(b), where the scaling power law follows an exponent $\gamma = 1$ at high repetition rates and has a discernable contribution of a $\gamma = 2$ process, presumably, related to the two-photon absorption, at 0.2 MHz. The linear plot (panel (a)) shows that at high repetition rates an interception of curves converges to the point with coordinates (0,0), which corroborates the linear character of polymerization mechanism.

The revealed linear scaling (Fig. 2) implies dominance of avalanche absorption or thermal polymerization (or both occurring together). Since the linear dependence is better obeyed at the high repetition rate, the thermal character of polymerization becomes dominant with increase of f . Thermal processes due to recombination of electrons created by the avalanche (which follows a linear power scaling [21]) and exothermic polymerization heat are both inseparable

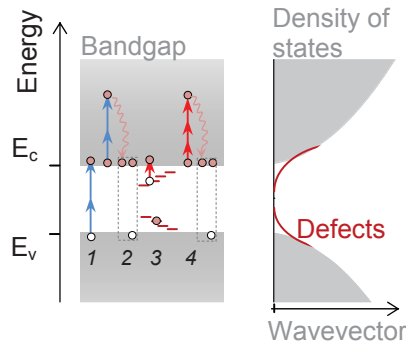


Fig. 4. Processes of light-matter interaction and ionization: (1) Two-photon absorption, (2) multiplication of electrons via avalanche ionization, (3) linear absorption seeding the avalanche by one-photon absorption from a defect or Urbach's tail state, (4) the avalanche rate $\propto \lambda^2$ [21] via long-wavelength seeding (process (3)). The processes shown here for electrons also take place for the holes (not shown for clarity). $E_{c,v}$ effective conduction and valence band energies of photo-material.

and defines the observed scaling with $\gamma = 1$. The seeding of avalanche has to be via nonlinear or defect-related absorption as in the case of fs-laser structuring [21]. At tight focusing, the two-photon absorption can even be excited by cw-laser illumination as shown by power law of photoluminescence [26]. In polymers, a local temperature increase is narrowing an efficient bandgap, J , of material and favors avalanche as $\sim 1/J$ [21]. The recombination rate is also faster at elevated temperatures and creates a positive feedback for polymerization by transferring energy into heat and a local temperature increase. Due to heat diffusion, which is faster than the scan speed, the pre-heated regions in front of the scanning point are “pre-conditioned” for seeding of polymerization. Direct absorption from shallow defects also directly provides seeding electrons for the avalanche and can even be more efficient than a nonlinear two-photon absorption as discussed below (see, Fig. 4). The mechanism described above explains recent observations of 3D polymerization by a cw-laser exposure [19] and is expected to be generic in resists and glasses [27]. It is consistent with laser recording of waveguides and optical elements in glasses and crystals [28–33]. The sub-wavelength structuring of photo-polymers, glasses, and crystals is possible even via processes, which show the single photon scaling ($\gamma = 1$), due to the threshold response of material for a particular modification, e.g., polymerization, densification/rarefaction of glass, etc.

In order to compare pulsed and cw-laser polymerization we estimate the cumulative dose of exposure, $D_{ac} = D_p \times N_p$ [J/cm²], where D_p is the dose-per-pulse defined by irradiance and pulse duration $I_p \tau_p$ [J/cm²] ($I_p = E_p / (\tau_p \pi w^2)$); for the cw-case $D_{ac} = P \times t_d / (\pi w^2)$ [J/cm²], here, P is power and $t_d = 2w/v$ is the dwell time required for beam to cross the focal spot at scanning speed, v . The same scaling exponent $\gamma = 1$ observed experimentally allows comparison of D_{ac} values over a wide range of polymerization conditions. In our case of sub-micrometer 3D structuring by 8 ps/532 nm/1 MHz at $v = 100 \mu\text{m/s}$ scan and $NA = 1.4$ focusing $D_{ac} \simeq 4.6 \text{ kJ/cm}^2$. In the case of cw-fabrication at the same wavelength [19], similar resolution structures are obtained at the power of $P \sim 10 \text{ mW}$, $v \sim 20 \mu\text{m/s}$, at $NA = 1.4$ focusing; then, one would find $D_{ac} \simeq 137 \text{ kJ/cm}^2$. The order of magnitude difference in the D_{ac} reflects less efficient use of a cw-laser delivered energy for nonlinear seeding of avalanche, hence, the most tight focusing $NA = 1.4$ has to be implemented.

Photo-materials can be optimized for more efficient seeding of avalanche, e.g., by direct

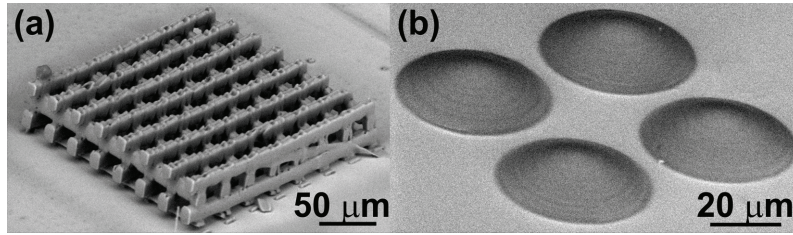


Fig. 5. 3D structures fabricated with 8 ps pulses at 1 MHz repetition rate: (a) a scaffold for cell growth and (b) microlens array. Structures were fabricated by 532 nm/8 ps pulses at 1 MHz repetition rate under $NA = 0.65$ (a) and $NA = 1.4$ (b) focusing, at 0.7 TW/cm^2 and 0.35 TW/cm^2 irradiance, respectively.

electron excitation from the defects (impurities or Urbach states) which would make a more efficient (linear) rather than non-linear absorption of optical energy. This is illustrated in Fig. 4, where it is shown that long wavelength excitation can seed the avalanche and radical generation for polymerization. Moreover, the avalanche rate scales with wavelengths as $\propto \lambda^2$ and, hence, is more efficient in chemical bond breaking (free electron excitation) as compared with nonlinear absorption which obeys $\propto 1/\lambda$ scaling [21]. Combination of, at least, two different wavelengths for seeding and driving avalanche, respectively, is yet another possibility to optimize laser polymerization or structuring of transparent materials by combined multi-photon and linear processes.

The light-matter interaction scenario outlined in Fig. 4 also explains why photopolymerization is not so wavelength sensitive if it is triggered by long wavelength ultra-short laser pulses. In the case of fs-pulses [21] of 150 fs/800 nm/1 kHz at $v = 100 \mu\text{m/s}$ scan and $NA = 1.4$ focusing results in $D_{ac} \simeq 7 \text{ J/cm}^2$ at irradiance $\sim 10 \text{ TW/cm}^2$. This small D_{ac} value signifies a more efficient energy use for polymerization in the case of fs-laser pulses as compared with ps- and cw-exposures. It is noteworthy, that thermal annealing is observed even at low repetition fs-direct write in chemically amplified SU-8 resist with strong exothermic effects [34]. For the high repetition rate, the condition $t_c = 1/f$ demarcates thermal accumulation and is defining the linear power scaling for higher frequencies as demonstrated here for ps-laser pulses.

3.2. Fabrication window: quality and fidelity of photo-polymerization

Since 3D photo-polymerization with high spatial resolution can be achieved with fs-, ps- or cw-laser pulses/beams at very different scanning speeds ranging from kHz, when thermal effects are minimized, to multi-MHz when they dominate, it is important to quantify the window of practical operation. For the parameter space varied in our experiments results are summarized in Fig. 3(a) by qualitative comparison of 3D photonic crystal structures. The best quality structures are retrieved under high repetition rate and for shorter pulses. This trend of $f \rightarrow \infty$ and $\tau_p \rightarrow 0$ shows strategy for good quality structures to be obtained. It can be rationalized as a precise energy delivery (a short pulse) and constant thermal conditions (high repetition rate) are required to control propagation of polymerization. The fidelity of 3D structuring can be defined by the fabrication window, $FW = \frac{P_d}{P_{th}}$, where P_d is the optical damage (a dielectric breakdown) power or irradiance and P_{th} is the polymerization threshold (see, Table 1). FW is a parameter characterizing processing throughput and flexibility: a higher FW means a possibility to change resolution in a wider range and is plotted in Fig. 3(b) for different τ_p and f . In the case of ultra-short pulses, a trend $FW(20 \text{ fs}) \simeq 2FW(200 \text{ fs})$ we have observed; the trend which could be expected from thermal diffusion which scales as $\propto \sqrt{\tau_p}$.

Table 1. Fidelity of 3D Fabrication^a

τ_p (ps)	8			16			25		
f (MHz)	0.2	0.5	1	0.2	0.5	1	0.2	0.5	1
P_{th} (TW/cm ²)	0.13	0.09	0.06	0.11	0.07	0.04	0.09	0.05	0.04
P_d (TW/cm ²)	0.39	0.28	0.20	0.22	0.16	0.11	0.16	0.11	0.096
P_b (TW/cm ²)	0.66	0.51	0.30	0.31	0.22	0.14	0.18	0.13	0.10
FW	3.0	3.1	3.3	2.0	2.3	2.8	1.8	2.2	2.4

^aThresholds of polymerization, P_{th} , optical damage, P_d , uncontrolled burning, P_b , and fabrication window,

$FW = \frac{P_d}{P_{th}}$ (for the irradiance), for SZ2080 photosensitized with THIO structured by pulses of duration τ_p at repetition rate, f .

When $\lambda = 1064$ nm, 8 ps pulse duration, and 1 MHz repetition rate was used to fabricate resolution bridges and photonic crystals, FW decreased approximately 1.5 times as compared to same conditions at 532 nm. Since avalanche ionization rate scales with wavelength as λ^2 there is a smaller margin for error before an uncontrolled optical breakdown occurs and is less controllable for the longer pulses [21]. Finally, the actual 3D structures polymerized at the optimized conditions, i.e., at high repetition rate using short ps-pulses are shown in Fig. 5. Micro-optical elements and 3D micro-scaffolds for cell growth and tissue regeneration can be fabricated by the direct laser write/cure using sol-gel organic-inorganic hybrid photopolymerizable materials.

4. Conclusions

It is demonstrated that ps-laser pulses at high repetition rate can be used to create 3D polymerized structures with resolution down to couple hundreds of nanometers. It is revealed that photopolymerization power law is linear at high repetition rates with larger values of the fabrication window, $FW > 2$; also, $FW > 2$ is observed for shorter 8 ps pulses facilitating high-fidelity fabrication of 3D nano-/micro-structures. Once thermal accumulation is present, i.e., when cooling time of focal volume is larger than time separation between pulses, $t_c > 1/f$, the linear scaling of a polymerized feature size on the dose per pulse has been observed.

Combination of lower cost ps-laser setup and high repetition rate is prospective for practical implementations of 3D polymerization in photonics, micro-optics and biomedicine since there is an efficient utilization of the delivered optical energy at low cost and a small footprint of laser setup. Alternatively, fs-lasers at high (and low) repetition rates make the most efficient polymerization in terms of the accumulated dose required for fabrication of 3D structures (however, at the highest cost of setup).

Acknowledgements

This work was supported by the Lithuanian Science Council grant MIP-10344 (Creation of Artificial Tissues for Regenerative Medicine) and EC's 7th Framework Programme (LASERLAB-EUROPE, grant No.228334, OPTOBIO). Authors thank Rokas Smilingis (Ekspla Ltd.) for technical assistance and Altechna Ltd. for providing Aerotech stages. SJ acknowledges support from Swinburne University of Technology for the startup funding of the Applied Plasmonics laboratory.